Computer-aided drug design and ADMET predictions for identification and evaluation of novel potential farnesyltransferase inhibitors in cancer therapy

ARTICLE *in* JOURNAL OF MOLECULAR GRAPHICS & MODELLING · FEBRUARY 2010

Impact Factor: 1.72 · DOI: 10.1016/j.jmgm.2009.11.011 · Source: PubMed

7 AUTHORS, INCLUDING:

Vinicius Barreto da Silva
Pontifícia Universidade Católica de Goiás (…
22 PUBLICATIONS **161** CITATIONS
SEE PROFILE

Fernanda Bononi
The University of Western Ontario
1 PUBLICATION **16** CITATIONS
SEE PROFILE

Carolina Benevenuto
University of São Paulo
5 PUBLICATIONS **24** CITATIONS
SEE PROFILE

Journal of Molecular Graphics and Modelling 28 (2010) 513–523

Contents lists available at ScienceDirect

Journal of Molecular Graphics and Modelling

journal homepage: www.elsevier.com/locate/JMGM

Computer-aided drug design and ADMET predictions for identification and evaluation of novel potential farnesyltransferase inhibitors in cancer therapy

Carlos Henrique Tomich de Paula da Silva [a], Vinicius Barreto da Silva [a], Jonathan Resende [a], Patrícia Franco Rodrigues [a], Fernanda Cristina Bononi [a], Carolina Gomes Benevenuto [a], Carlton Anthony Taft [b,*]

[a] Departamento de Ciências Farmacêuticas, Faculdade de Ciências Farmacêuticas de Ribeirão Preto, Universidade de São Paulo, Av. do Café, s/n, Monte Alegre, 14040-903, Ribeirão Preto-SP, Brazil
[b] Centro Brasileiro de Pesquisas Físicas, Rua Dr. Xavier Sigaud, 150, Urca, 22290-180, Rio de Janeiro-RJ, Brazil

ARTICLE INFO

Article history:
Received 9 October 2009
Received in revised form 29 November 2009
Accepted 30 November 2009
Available online 4 December 2009

Keywords:
Farnesyltransferase
Cancer
Drug design
Virtual screening
ADMET predictions

ABSTRACT

We have used various computational methodologies including molecular dynamics, density functional theory, virtual screening, ADMET predictions and molecular interaction field studies to design and analyze four novel potential inhibitors of farnesyltransferase (FTase). Evaluation of two proposals regarding their drug potential as well as lead compounds have indicated them as novel promising FTase inhibitors, with theoretically interesting pharmacotherapeutic profiles, when compared to the very active and most cited FTase inhibitors that have activity data reported, which are launched drugs or compounds in clinical tests. One of our two proposals appears to be a more promising drug candidate and FTase inhibitor, but both derivative molecules indicate potentially very good pharmacotherapeutic profiles in comparison with Tipifarnib and Lonafarnib, two reference pharmaceuticals. Two other proposals have been selected with virtual screening approaches and investigated by us, which suggest novel and alternatives scaffolds to design future potential FTase inhibitors. Such compounds can be explored as promising molecules to initiate a research protocol in order to discover novel anticancer drug candidates targeting farnesyltransferase, in the fight against cancer.

1. Introduction

Ras protein is a cell component that controls growth and multiplication. These are small G proteins, that are linked to GDP in rest, and linked to GTP when active, whereas the linkage to GTP is temporary. It was previously observed that an abnormal form of the signaling Ras is present in almost 30% of cancers, being more prevalent in both pancreatic and colon cancer [1,2]. This protein binds in a persistent manner to GTP and cannot promote hydrolysis, as occurs normally, being thus constantly activated. It is believed that once the Ras proteins are involved in the control of the cell growth and divisions, mutations of these proteins could be related to the development of cancer. Thus, methods capable of neutralizing Ras would be considered useful in the fight against cancer. In this context, protein farnesyltransferase (FTase) has been studied as a therapeutic target [3].

Ftase enzyme was primarily identified in 1990, in a large number of species, including mammals [1–4], fungi [5], plants [6,7] and protists [8]. This enzyme has proven to be essential for these organisms, whereas the elimination resulted in severe defects or lethality [1–5]. FTase is a zinc metaloenzyme that catalyzes the first and crucial step in a series of post-translational modifications that indicate the localization of the membrane proteins — the transfer of a farnesyl group of the diphosphate-farnesyl molecule (FPP) to cystein, present in the C-terminal of a array of proteins containing the conserved CAAX motif (C = cystein, A = aliphatic amino acid, X = any other amino acid), present, for example, in the Ras proteins. Farnesylation is obligatory for H-Ras, as well as a large amount of small molecules capable of inhibiting this enzyme, developed as anticancer agents [9–11].

The accepted mechanism for farnesyltransferase is of high complexity. First, the FPP binds to FTase, forming a complex FPP–enzyme, followed by the association with the tail CAAX, forming the enzyme–FPP–CAAX peptide complex [12,13]. After formation of the thioeter, the modified peptide continues to be associated with FTase in a complex enzyme-product [13,14]. Dissociation of the farnesylated product is facilitated by the binding with another FPP molecule or another peptide substrate (CAAX) [14].

The farnesyltransferase inhibitors were initially developed with intent to neutralize *Ras* in cancers, where it was observed a large

* Corresponding author. Tel.: +55 21 2141 7201; fax: +55 21 2141 7201.
E-mail address: catff@terra.com.br (C.A. Taft).

1093-3263/$ – see front matter © 2009 Elsevier Inc. All rights reserved.
doi:10.1016/j.jmgm.2009.11.011

incidence of mutations in *Ras*. Nonetheless, of the four molecules initially developed, only two continue to be available: Tipifarnib (Zarnestra, R11577) and Lonafarnib (Sarasar, SCH 66336). Tipifarnib is a selective inhibitor orally active that inhibits the proliferation of a great variety of human tumor cells, in vivo and in vitro [15,16]. Such as Tipifarnib, Lonafarnib — a tricycle inhibitor, is also orally active in Ras-dependent and Ras-independent malignant tumors [17,18]. The anti-tumoral activity was demonstrated in various preclinical models, whereas phase-I studies demonstrated that doses up to 200 mg are safe and well tolerated [19].

Many farnesyltransferase inhibitors are in a number of phase-I, -II and -III clinical tests for the treatment of cancer, but the response of the patients was not significant [11,20]. A plausible explanation for such absence of efficacy would be the alternative prenylation process, where some substrates of farnesyltransferase are recognized by Type-I Geranyltransferase (GGTase-I), when the activity of protein farnesytransferase is at the limit [11,21].

An increasing number of computational works have been addressed recently to investigate many diseases such as cancer regarding a therapeutic target as well as inhibitors [22–27]. This present work searches for new inhibitors of farnesyltransferase, and suggests potential novel FTase inhibitors with highest activities or a large number of interactions with the target, leading to a greater specificity. We have investigated these proposals regarding low toxicity and good oral bioavailability. Structures of the most active leads reported in literature were used and results obtained indicate novel promising FTase inhibitors with theoretically good pharmacotherapeutic profile.

2. Computational details

FTase structures in complex with Lonafarnib and Tipifarnib (PDB codes 1O5M and 1SA4, respectively), as well as another very active inhibitor (L-778123 — PDB code 1S63), were selected from Protein Data Bank. These three inhibitors were used to propose novel derivatives by rational molecular modifications, based on physicochemical and pharmacokinetic properties. For calculation of the properties, *DS ViewerPro 5.0* software [28] and the web server *ADME/TOX WEB* (http://pharma-algorithms.com/webboxes/) were used. Activity predictions were performed with the web server *PASS* (Prediction of Activity Spectra for Substances, at http://195.178.207.233/PASS/index.html) [29], which predicts the biological activity spectrum for a compound on the basis of its structural formula. *PASS* Inet predictions include 4535 pharmacological effects, mechanisms of action, mutagenicity, carcinogenicity, teratogenicity and embryotoxicity [29].

Synthetic accessibility was addressed using the web version of the *SYLVIA* software (at http://www.molecular-networks.com/online_demos/sylvia/) [30], whereas toxicology predictions were performed using an expert system, the *DEREK 10.0.2* software [31].

Flexible docking and virtual screening simulations were performed using *GOLD 4.1.1* software [32]. *GOLD* performs flexible docking using a genetic algorithm, which was originally optimized from a set of 305 complexes structures with coordinates deposited in PDB. We used populations of 100 conformers, 100,000 operations, 95 mutations and 95 crossovers. For virtual screening, two orientations of highest score were selected for each of the best 50 compounds ranked in the structures database by the score function GoldScore. Based on this function, the software classifies the orientations of the molecules by a decreasing ordering of affinity with the binding site of FTase. Molecules obtained by this virtual screening approach were assessed individually for rescoring and re-ranking. The proposed compounds, here modeled by molecular modifications of three very active FTase inhibitors, were optimized at B3LYP/6-31G* level of calculation using *Gaussian 03* software [33].

For virtual screening simulations, the collection of compounds Kinaset from the ChemBridge database was used. Two docking simulations were initially performed with Tipifarnib and Lonafarnib in order to validate the original crystallographic coordinates of the inhibitors. For docking of Lonafarnib, 10 solutions of genetic algorithm were investigated, allowing premature termination if the root mean square deviation (RMSD) amongst three solutions (orientations) was less than 1.5 Å. Calculations were performed inside a sphere of 12 Å radius centered at carbon beta of the W106 side chain of the FTase–Lonafarnib complex structure downloaded from PDB (PDB code 1O5M). For docking of Tipifarnib, 10 solutions of genetic algorithm were similarly investigated, allowing premature termination if the root mean square deviation amongst three solutions (orientations) was less than 1.5 Å. Calculations were performed inside a sphere of 12 Å radius centered at carbon beta of the W106 side chain of the FTase–Tipifarnib complex structure downloaded from PDB (PDB code 1SA4). For docking and virtual screening simulations, all the ligands and waters were removed, except farnesyl diphosphate (FPP) and the catalytic zinc.

Molecular interaction fields studies were performed with the FTase–Tipifarnib complex structure (PDB code 1SA4), using *GRID v2.2* software [34]. The electrostatic and van der Waals potentials are computed for interaction energy between chemical probes and atoms of a selected region of the FTase, a conservative box where the Poisson equation is solved. Three prototypical probe groups were used: DRY, aromatic Csp^2 carbon and chlorine, which were placed in a 0.33 Å spacing grid covering the overall binding site.

Molecular dynamics simulations (MD) were performed with FTase and two best proposals selected by virtual screening, using the discover module of the *Insight II* package [35]. Previously, the energies of the complexes were minimized using 1000 steps of a combined steepest-descent/conjugate gradient algorithm and the Discover/CVFF force field of *Insight II*. Implicit solvent conditions with a dielectric constant of 80 (water) were employed. No constraints were made during any optimization procedure. Subsequently, 1500 ps MD simulations of the two complexes were carried out with an equilibration phase of 80 ps, at 298 K. The NBO partial atomic charges of the molecules, calculated at the B3LYP/6-31G* level, were used, and the atomic charges for the receptor atoms were obtained using an all atom force field CVFF. The coordinates of the two systems were saved every 1.5 ps during the simulations. From the molecular trajectories generated by the MD simulations, the root mean square deviations of selected FTase-inhibitor contacts were analyzed, as well as the total energy as a function of time.

3. Results and discussion

3.1. Physicochemical and pharmacokinetic properties analyses

As a preliminary step in this work toward a rational design of novel potential farnesyltransferase inhibitors, we have investigated relevant physicochemical properties including the Lipinski's Rule of Five (RO5) [36] of several very active and most cited FTase inhibitors that have activity data reported and are launched drugs (two compounds) or in clinical tests (four compounds). The aim is to search for significant correlation between one or more properties and the biological activity reported for these six inhibitors. We have investigated SCH 226734, R115777 (Tipifarnib), SCH 66336 (Lonafarnib), BMS-214662, L-778123 and U49.

SCH 226734 and SCH 66336 are members of a known class of tricyclic noncytotoxic compounds with anticancer activity [37,38]. R115777 and BMS-214662 have been developed by the Jansen Research Foundation and Bristol-Myers Squibb, respectively [39]. R115777 is a nonpeptide quinolone analogue, and the first FTase inhibitor to be launched in the market. BMS-214662 is a

nonpeptide tetrahydrobenzodiazepine compound and, such as Tipifarnib, it is selective toward protein farnesyltransferase, showing no activity against protein geranylgeranyltransferase type I (GGTase-I) [39].

Protein prenyltransferase inhibitors must be very specific toward one prenylation enzyme, because preclinical studies indicate that inhibition of both FTase and GGTase-I may be toxic [39]. L-778123, a nonpeptide inhibitor, is nonselective toward FTase, however inhibits this enzyme and GGTase-I by different binding modes [40]. In FTase, L-778123 binds in the peptide-binding site, whereas in GGTase-I, it binds in the lipid-binding site, suggesting different mechanisms of action regarding these two enzymes, whose difference remains less understood [40]. U49 is a nonpeptide FTase inhibitor containing a macrocyclic aminopyrrolidinone scaffold [41]. Structures are depicted in Fig. 1.

With the exception of SCH 226734, all the molecules here investigated have structures deposited in PDB, in complex with FTase: R115777 (PDB code 1SA4), SCH 66336 (PDB code 1O5M), BMS-214662 (PDB code 1SA5), L-778123 (PDB code 1S63) and U49 (PDB code 1LD8). We have used such bioactive conformations reported for these five inhibitors as well as a minimum local energy structure of SCH 226734 to initially calculate the properties of the Rule of Five, as well as the following physicochemical properties: molecular volume, molecular refractivity, surface area, mean polarizability, HOMO and LUMO energies, and total dipole. These selected properties can be divided in three groups including the main features or intermolecular forces involved in the ligand binding process, such as polar and hydrophobic interactions, as well as shape/topology adjustment. Results are shown in Tables 1 and 2.

According to Table 1, only SCH 226734 violates the rule in more than 1 property ($\log P$), indicating a likely poor absorption. Analyzing the properties depicted in Table 2 and their correlation (R^2) with the biological activity ($-\log IC_{50}$), we have found values of R^2 of 0.84 for $\log P$, 0.67 for molecular refractivity, 0.65 for polarizability and 0.60 for molecular volume. No correlation was observed between any electronic properties, related to polar interactions, and the biological activity. Results point out the likely role of the lipophilicity as well as the shape of the compounds to achieve highest activity, suggesting the importance to design novel FTase inhibitors with similar shapes and volumes to these six reported compounds, as well as $\log P$ value close to the limit of 5 regarding to the RO5.

In addition to the physicochemical properties, and in order to investigate where is it possible to improve the pharmacotherapeutic profiles of Tipifarnib or Lonafarnib, we have calculated pharmacokinetic properties for these compounds via the web server *ADME/TOX WEB*.

For Tipifarnib, the oral bioavailability (%*F*) is estimated between 30% and 70%, and its solubility in water is moderate (slightly soluble), with Sw > 1 mg/mL (99% of probability). Such FTase inhibitor is also predicted to be chemically stable in acidic conditions (pH < 2) and shows a theoretically low passive absorption across intestinal barrier, with maximum passive absorption of 2%, and no active transport is predicted for such a molecule.

For this compound, no significant first-pass metabolism in liver and/or intestine is predicted, and such a molecule also shows high probability to bind plasmatic proteins (%PPB = 98.1%). It is a weak base (base $pK_a < 8.5$). These drugs predominantly bind to alpha1-acid glycoprotein and albumin. The volume of distribution (V_d) predicted for this compound is 4.02 L/kg, and it is classified as a hydrophilic or moderately hydrophobic basic drug (no acid groups with $pK_a < 7.5$, base $pK_a > 7$, and $\log P < 3.5$). Drugs in this group have highly variable V_d values (0.2–20 L/kg).

P-gp (P-glycoprotein) inhibitor probability for Tipifarnib is 85.3%, being classified as a possible inhibitor since such molecule is a large amphiphilic base. It is also possible that this compound could be a substrate of such glycoprotein (MW > 400, large H-acceptor), with a probability of 70.5%. However, regarding a high-affinity P-gp substrate probability (significant efflux in vivo), it shows a relatively small value (33.2%).

For Lonafarnib, the oral bioavailability (%*F*) is estimated between 30% and 70%, and its solubility in water very low (highly insoluble), with Sw < 0.1 mg/mL (98.5% of probability). Such FTase inhibitor is also predicted to be chemically stable in acidic conditions (pH < 2) and shows theoretically high passive absorption across intestinal barrier (>70%), and maximum passive absorption of 100%. No active transport is predicted for such molecule.

For this compound, no significant first-pass metabolism in liver and/or intestine is predicted, and such molecule also shows high probability to bind plasmatic proteins (%PPB = 99.6%). It is a weak base (base $pK_a < 8.5$). These drugs predominantly bind to alpha1-acid glycoprotein and albumin. The volume of distribution (V_d) predicted for this compound is 3.47 L/kg, and it is classified as a hydrophobic neutral drug (no acid groups with $pK_a < 7.5$, no base groups with pK_a value > 7, and $\log P > 1$). Most of the drugs in this group have moderate V_d values (90% of values are in the range of 0.5–10 L/kg). V_d can be larger for very hydrophobic drugs.

P-gp inhibitor probability for Lonafarnib is 93.9%, being classified as a possible inhibitor once such molecule is a large hydrophobic base. It is also classified as a P-gp substrate (MW > 550, large H-acceptor, amide groups, aliphatic cycles). In addition, regarding a high-affinity P-gp substrate probability (significant efflux in vivo), it shows a significant value of 47.9%.

With the exception of absorption, all of the pharmacokinetic properties calculated for Tipifarnib are more consistent with a better pharmacotherapeutic profile, in comparison with Lonafarnib. Tipifarnib has also more affinity with farnesyltransferase than Lonafarnib, which is well correlated with $\log P$ as well as shape properties and van der Waals interactions (Tables 1 and 2). According to the important role of van der Waals interactions here suggested by the calculations of the physicochemical properties, novel compounds must additionally retain aromatic pharmacophoric groups common to the FTase inhibitors.

Thus, a possible strategy to design novel FTase inhibitors would be to modify the structure of Tipifarnib, optimizing absorption with slightly more lipophilic structures. Molecular modifications can be rationally performed *in silico*, thus guided by chemical inspection and superposition of the available crystallographic enzyme–inhibitor complexes as well as molecular interaction fields (MIFs) studies performed with an aromatic probe inside the farnesyltransferase active site.

3.2. Molecular interaction fields studies

In Fig. 2A, superposition between the FTase–Tipifarnib and FTase–Lonafarnib crystallographic complexes is shown in phase with MIFs calculated using the DRY (hydrophobic), aromatic Csp^2 and chlorine probes. In Fig. 2B, superposition between the FTase–Tipifarnib and FTase–L-778123 crystallographic complexes is shown in phase with molecular interaction fields calculated using the same three probes. Superposition of Tipifarnib with Lonafarnib and L-778123, as well as MIFs obtained with the DRY (hydrophobic) and aromatic Csp^2 probes, suggests the important role of the imidazol, quinolinone and chloro-benzene rings of Tipifarnib in the high affinity of this compound for FTase. The chloro-benzene and imidazol rings are similarly found in Lonafarnib or L-778123, at the same binding sites. In addition, MIFs point out the binding sites of aromatic rings and hydrophobic groups, suggesting a replacement

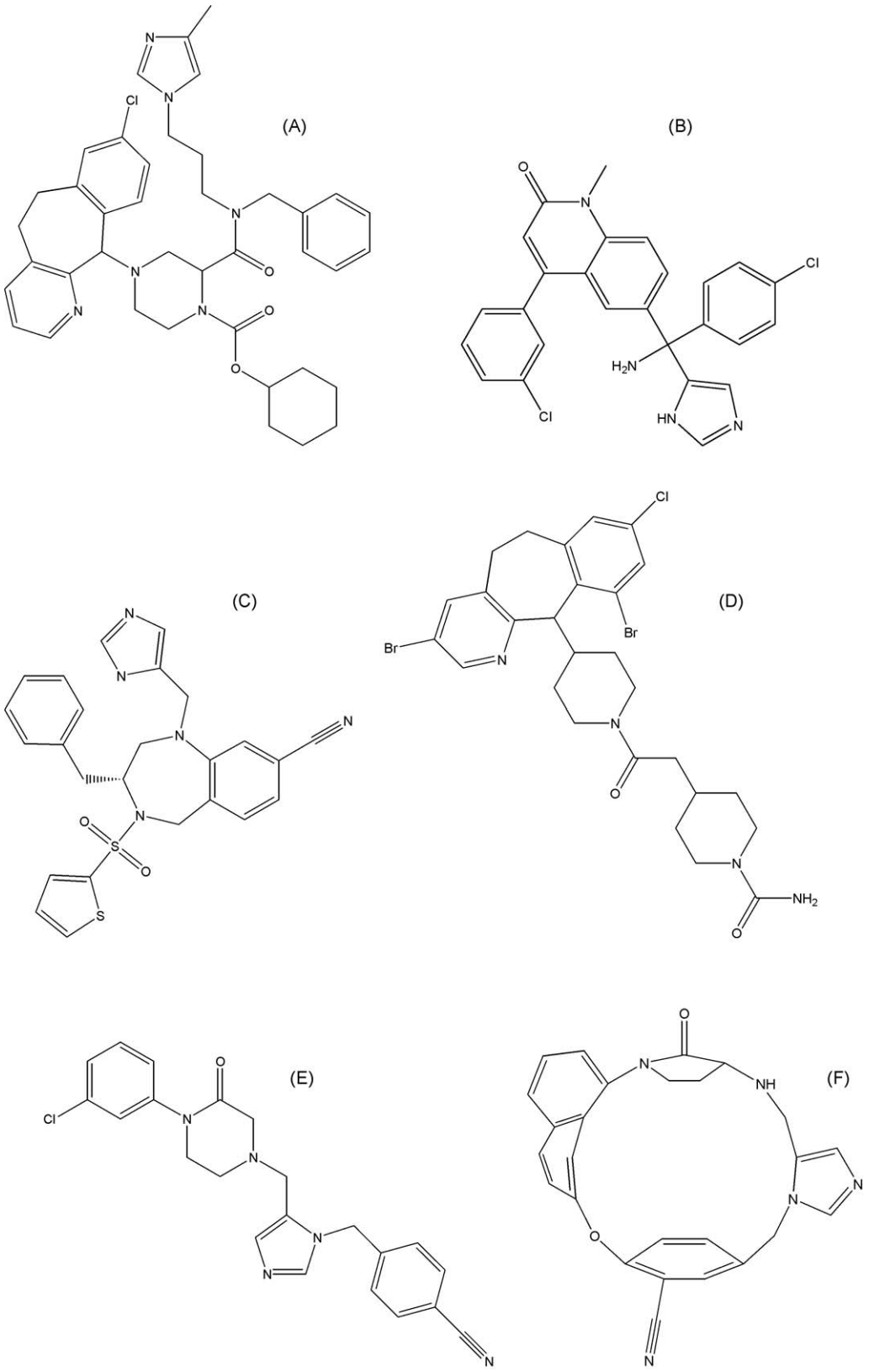

Fig. 1. Structures of six very active and most cited FTase inhibitors that have activity data reported: (A) SCH 226734, (B) R115777 (Tipifarnib), (C) BMS-214662, (D) SCH 66336 (Lonafarnib), (E) L-778123 and (F) U49.

of the oxygen atom present in the quinolinone moiety of Tipifarnib by a hydrophobic atom/group. Such molecular modification could result in a better fit of the inhibitor inside the FTase active site, contributing to stabilize the binding of such molecule, favoring the formation of a covalent bond with zinc atom, via its imidazol ring.

Another modification suggested by these energetic studies would be the replacement of chlorine by other isostere in the

Table 1
Biological activities and properties of the Rule of Five of six most cited FTase inhibitors, launched or in clinical tests.

Inhibitor	pIC_{50}	Molecular weight	H-bond acceptors	H-bond donors	log *P*	RO5 violations
SCH 226734	9.44	695.38	6	0	6.79	2
Tipifarnib	9.22	491.45	3	2	5.06	1
BMS-214662	8.85	489.65	5	1	4.05	0
Lonafarnib	8.72	638.87	3	1	4.79	1
L-778123	8.48	405.92	4	0	2.94	0
U49	8.45	435.52	5	1	2.70	0

Table 2
Physicochemical properties calculated for 6 most cited FTase inhibitors.

Inhibitor	Molecular volume (Å^3)	Molecular refractivity (Å^3)	Surface area (Å^2)	Mean polarizability (Å)	E_{LUMO} (eV)	E_{HOMO} (eV)	Total dipole (Debye)
SCH 226734	540.86	196.16	762.02	91.20	−0.24	−9.05	11.50
Tipifarnib	356.81	138.61	467.66	61.66	−0.63	−7.56	3.83
BMS-214662	351.78	135.21	499.57	62.17	−1.70	−8.95	7.51
Lonafarnib	410.69	149.41	561.47	63.51	−0.23	−9.25	4.88
L-778123	302.53	113.41	421.19	50.36	−0.75	−9.17	4.01
U49	320.77	124.56	438.02	58.69	−1.15	−8.54	8.47

chloro-benzene ring. MIFs due to the chlorine probe suggest an extension of the position of this group in order to achieve the most energetic chlorine binding site, whereas MIFs due to both the hydrophobic and aromatic probes signalize the importance of maintaining or increasing the number of hydrophobic interactions with FTase, at this selected region of the active site.

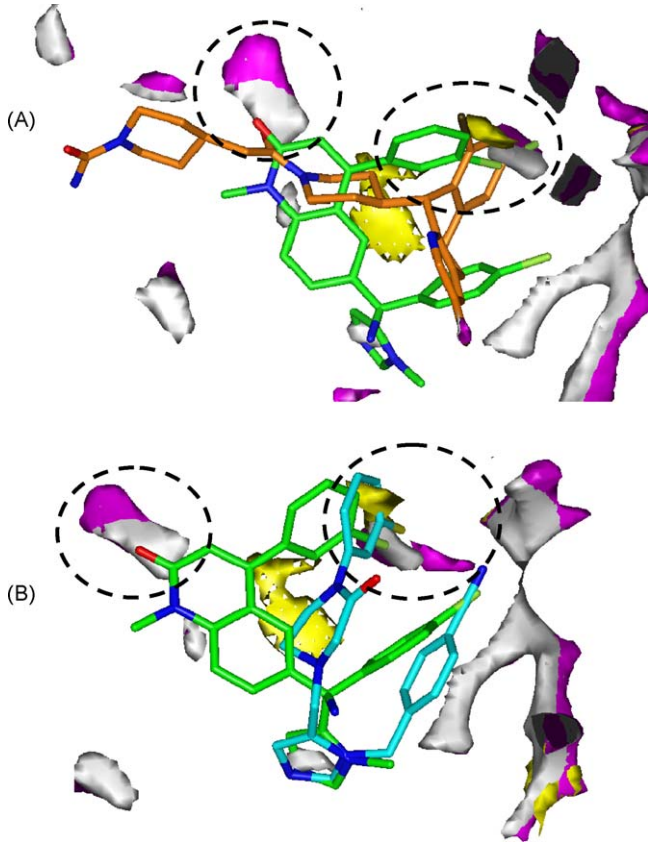

Fig. 2. In (A), superposition between the FTase–Tipifarnib (carbon atoms in green) and FTase–Lonafarnib (carbon atoms in orange) crystallographic complexes is shown in phase with MIFs calculated using the DRY (MIFs in yellow, energy contoured at – 1.5 kcal/mol), aromatic Csp^2 (MIFs in light grey, energy contoured at – 2.7 kcal/mol) and chlorine (MIFs in magenta, energy contoured at – 4.5 kcal/mol) probes. In (B), superposition between the FTase–Tipifarnib and FTase–L-778123 crystallographic complexes is shown in phase with molecular interaction fields calculated using the same three probes. Selected dashed circles show important regions that could be explored to design novel FTase inhibitors. (For interpretation of the references to color in this figure legend, the reader is referred to the web version of the article.)

In light of these findings, we propose two novel Tipifarnib analogues. Our so called Proposal 1 has a cyanide group in substitution to the chlorine in the chloro-benzene ring, as well as an isosteric replacement of the quinolinone ring by a quinoline moiety, which contains a methyl group in substitution to the oxygen atom (Fig. 3). Our so called Proposal 2 has a cyanide group in substitution to the chlorine in the chloro-benzene ring, as well as an isosteric replacement of the quinolinone ring by a methyl-naphthalene moiety (Fig. 3).

3.3. Docking simulations of the drugs

In order to propose binding modes for these proposals, we have initially performed docking simulation with Tipifarnib, using the FTase–Tipifarnib crystallographic complex (PDB code 1SA4). Crystallographic orientation of Tipifarnib has been reproduced (RMSD of 0.66 Å), with score of 59.1 for the top-ranked solution, thus validating such docking approach for FTase complexes (Fig. 4).

Once optimized the GOLD parameters for FTase and inhibitors, we have performed docking simulations for our two molecules proposed, with scores of 78.3 and 78.9 for respective top-ranked solutions of proposals 1 and 2. Results are shown in Fig. 5. Both proposals 1 and 2 have cyanide in substitution of chlorine in the chloro-benzene ring, making available a more extensive and strong net of van der Waals contacts (including dipole-induced dipole interactions) with W102 and W303 residues as well as the farnesyl diphosphate substrate. The extent of induction of dipole depends on the polarizability of the apolar molecule/group. Polarizability, as a measure of the propensity of the electrons to be displaced by external fields, is here favored due to the larger size of the tryptophan residues, whose electron cloud is softer and more deformable. In fact, it is well established that FTase inhibitors in general require FPP to form a high-affinity complex with FTase, where this substrate must be first bound to enzyme [39].

Regarding Proposal 1, the replacement of the quinolinone ring by a quinoline moiety, which contains a methyl group in substitution to the oxygen atom, makes available an additional van der Waals contact between such methyl group and L96, increasing the affinity of the proposal for FTase.

Regarding Proposal 2, the same interaction could be available involving a methyl group present in this molecule, but such proposal is additionally more lipophilic than Proposal 1 due to the naphthalene moiety, in an attempt to improve absorption. Our

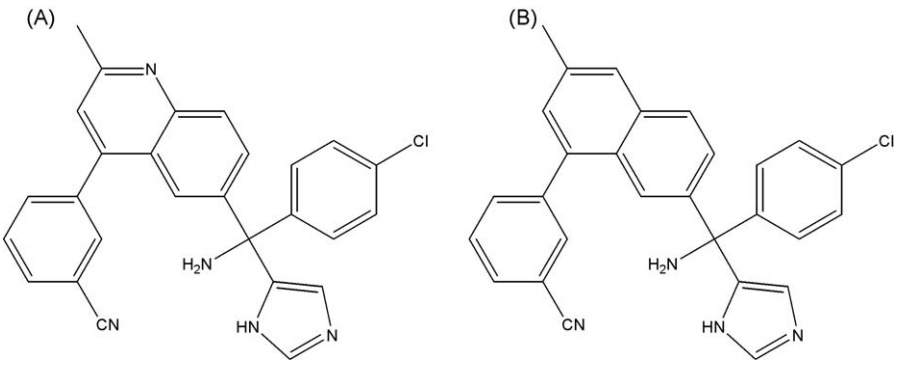

Fig. 3. Structures of novel potential FTase inhibitors here proposed. In (A), Proposal 1: 3-{6-[Amino-(4-chloro-phenyl)-(3*H*-imidazol-4-yl)-methyl]-2-methyl-quinolin-4-yl}-benzonitrile; in (B), Proposal 2: 3-{7-[amino-(4-chloro-phenyl)-(3*H*-imidazol-4-yl)-methyl]-3-methyl-naphthalene-1-yl}-benzonitrile.

proposals are supported by the knowledge that Tipifanib and analogues are only ~60% buried by the protein and adjacent FPP molecule [39]. This may permit addition of functional groups for modulation of bioavailability, toxicity and stability without affecting drug binding or specificity.

3.4. Pharmacokinetic profiles of the proposals

In this context, we have calculated physicochemical and pharmacokinetic properties for our proposals. Proposal 1 and Proposal 2 have molecular weights of 463.1 and 462.2, respectively, whereas the corresponding value obtained for Tipifarnib is 491.5. Our first proposal has a log *P* of 5.5, slightly higher than the value calculated for Tipifarnib (5.06), whereas Proposal 2 has a log *P* of 6.24. Mean polarizability is 65.3 for Proposal 1, and 66.4 for Proposal 2, values slightly higher than the calculated for Tipifarnib (61.7). Molecular volume calculated for Proposal 1 is 354.9, whereas for Proposal 2 and Tipifarnib the corresponding values are 357.26 and 356.8, respectively. Molecular refractivity is 136.0 for Proposal 1, and 138.6 for both Proposal 2 and Tipifarnib.

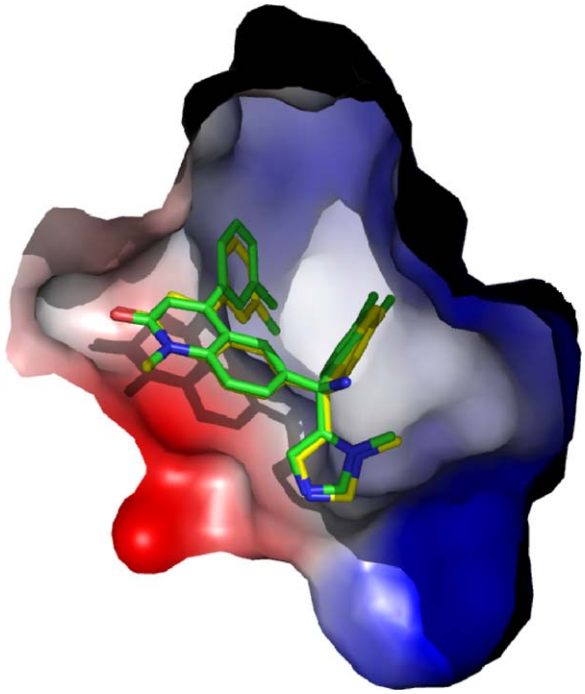

Fig. 4. Superposition between the crystallographic structure of Tipifarnib (carbon atoms in green) and the top-ranked docking solution of Tipifarnib (carbon atoms in yellow), inside the farnesyltransferase active site (represented as an electrostatic potential surface) is shown.

Properties well correlated with the affinity of inhibitors for protein farnesyltransferase, such as MV, MR MP and log *P*, show values close or slightly higher than the calculated for Tipifarnib, the most potent FTase inhibitor launched in the market. Such as previously discussed, the aim is to propose novel FTase inhibitors with similar shapes and volumes to these reported six compounds, trying to increase the affinity for the enzyme and, if possible, to improve the pharmacotherapeutic profile of Tipifarnib or Lonafarnib.

Following this idea, we have calculated pharmacokinetic properties for our candidates. For Proposal 1, the oral bioavailability (%*F*) is estimated between 30% and 70%, and its solubility in water is moderate (slightly soluble), with Sw > 1 mg/mL (99% of probability). Such an FTase inhibitor is also predicted to be chemically stable in acidic conditions (pH < 2) and shows a theoretically good passive absorption across intestinal barrier (>70%), and maximum passive absorption of 100%. No active transport is predicted for such a molecule.

For this our proposal, no significant first-pass metabolism in liver and/or intestine is predicted, and such proposal also shows high probability to bind plasmatic proteins (%PPB = 98.9%). It is a weak base (base pK_a < 8.5). These drugs predominantly bind to alpha1-acid glycoprotein and albumin. The volume of distribution (V_d) predicted for this compound is 4.19 L/kg, and it is classified as a hydrophilic or moderately hydrophobic basic drug (no acid groups with pK_a < 7.5, base pK_a > 7, log *P* < 3.5). Most of drugs in this group have moderate or high V_d values (90% of these values are greater than 1 L/kg, and 50% are greater than 10 L/kg).

P-gp inhibitor probability for Proposal 1 is 88.6%, being classified as a possible inhibitor once such molecule is a large amphiphilic base (pK_a < 7, no acid groups, MW > 360). It is also classified as a possible substrate of such glycoprotein (MW > 400, large H-bond acceptor), with a probability of 58.0%. However, regarding a high-affinity P-gp substrate probability (significant efflux in vivo), it shows a relatively small value (26.0%).

For Proposal 2, the oral bioavailability (%*F*) is estimated between 30% and 70%, and its solubility in water is moderate (slightly soluble), with Sw > 1 mg/mL (99.3% of probability). Such FTase inhibitor is also predicted to be chemically stable in acidic conditions (pH < 2) and shows a theoretically good passive absorption across intestinal barrier (>70%), and maximum passive absorption of 100%. No active transport is predicted for such molecule.

For our proposal, no significant first-pass metabolism in liver and/or intestine is predicted, and such proposal also shows high probability to bind plasmatic proteins (%PPB = 99.8%). It is a weak base (base pK_a < 8.5). These drugs predominantly bind to alpha1-acid glycoprotein and albumin. The volume of distribution (V_d)

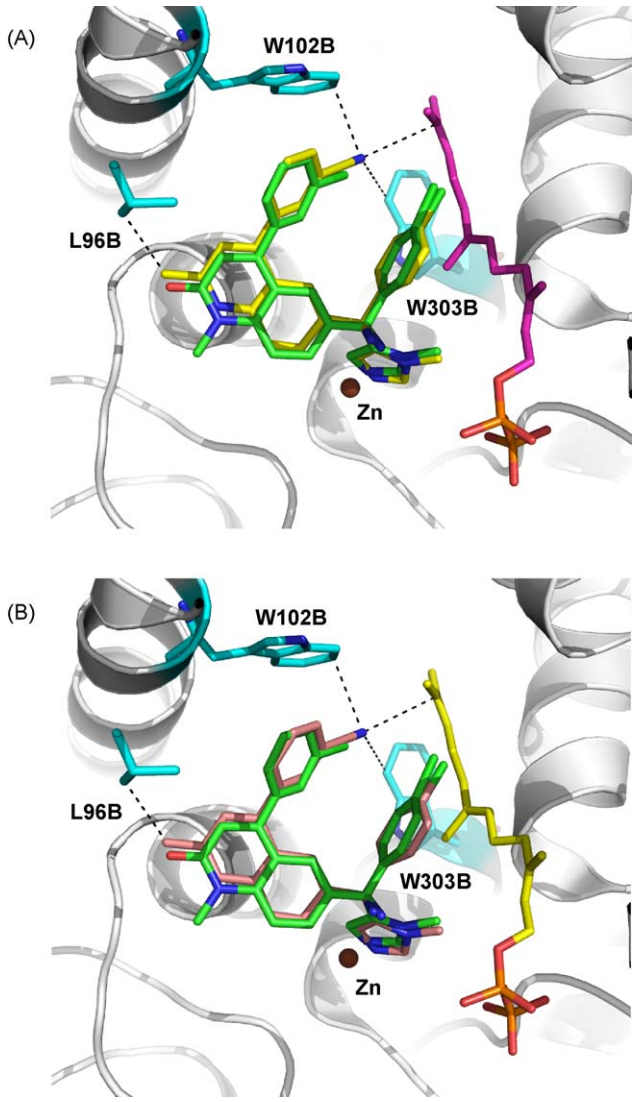

Fig. 5. In (A), superposition between the crystallographic structure of Tipifarnib (carbon atoms in green) and the top-ranked docking solution of Proposal 1, a Tipifarnib-based potential FTase inhibitor (carbon atoms in yellow), is shown. The crystallographic farnesyl diphosphate (FPP) structure is represented with carbon atoms in magenta. Important additional van der Waals interactions are established between the Proposal 1 and the active site (selected residues are shown with carbon atoms in cyan). In (B), superposition between the crystallographic structure of Tipifarnib (carbon atoms in green) and the top-ranked docking solution of Proposal 2, another Tipifarnib-based potential FTase inhibitor (carbon atoms in light brown), is shown. The crystallographic farnesyl diphosphate (FPP) structure is represented with carbon atoms in yellow. Important additional van der Waals interactions are established between the Proposal 2 and the active site (selected residues are shown with carbon atoms in cyan). (For interpretation of the references to color in this figure legend, the reader is referred to the web version of the article.)

predicted for this compound is 6.16 L/kg, and it is classified as a moderately hydrophobic basic drug (no acid groups with $pK_a < 7.5$, base $pK_a > 7$, $\log P < 3.5$).

P-gp inhibitor probability for Proposal 2 is 89.4%, being classified as a possible inhibitor once such molecule is a large amphiphilic base ($pK_a < 7$, no acid groups, MW > 360). It is also classified as a possible substrate of such glycoprotein (MW > 400, large H-bond acceptor), with a probability of 59.1%. However, regarding a high-affinity P-gp substrate probability (significant efflux in vivo), it shows a relatively small value (26.3%).

Analyzing the results obtained for our two candidates, both proposals 1 and 2 are relatively soluble and show good passive absorption across intestinal barrier compared to Tipifarnib. Evaluating the lipophilicity, Proposal 1 shows a log *P* value comparable to the calculated for Tipifarnib, whereas Proposal 2 is slightly distant (6.24) of the limit value of 5 (according to the Rule of Five).

Comparable high probabilities to bind plasmatic proteins were also obtained for our two proposals as well as Tipifarnib. The binding properties are computed from physicochemical properties (lipophilicity, ionization constants and hydrogen-bonding capacity) as well as structural descriptors of the compounds. In general, it is assumed that only free drug can cross membranes and bind to the intended molecular target [42], and it is therefore important to estimate the fraction of drug bound to plasma proteins.

For a compound crossing a membrane by purely passive diffusion, a reasonable permeability estimate can be made using single molecular properties, such as partition and distribution coefficients or hydrogen-bonding capacity. However, besides the purely physicochemical component contributing to membrane transport, many compounds are affected by biological events, including the influence of transporters and metabolism [42].

Many drugs are substrates for transporter proteins, which can either promote or hinder permeability. In particular, P-glycoprotein is the most widely known efflux transporter, having a great effect on the success of drug discovery projects. P-gp was initially identified as a major cause of resistance by cancer cells to multiple drugs (e.g. paclitaxel, etoposide) having a variety of structures. A major oncology discovery strategy has been to test lead compounds for their ability to overcome multidrug resistance in cell lines that are highly drug resistant through the expression of high levels of this glycoprotein [43], and in the context of our cancer's work, P-gp specificity plays an important role.

As for other properties, rules are useful as a guide for the initial assessment of a compound, based on its structure. Rules for P-gp are commonly referred to as "Rule of 4", where increasing numbers of hydrogen bond acceptors (N + O atoms $\geq$8) as well as molecular weight greater than 400 appear to confer increasing likelihood of P-gp efflux [43]. In addition, it has been shown that compounds with N + O = 4 have a 33% chance of being effluxed by P-gp, whereas compounds with N + O = 6 have a 65% chance. Our proposals have N + O = 5 (Proposal 1) and N + O = 4 (Proposal 2), similar or slightly more favorable than Tipifarnib (with N + O = 5). Proposals 1 and 2 were designed in order to have decreased H-bond acceptor potential as a strategy to reduce P-gp efflux.

Also slightly greater and favorable are the V_d values predicted for Proposal 1 (4.19) and Proposal 2 (6.16), in comparison with the values calculated for Tipifarnib (4.02) and Lonafarnib (3.47). Volume of distribution is a theoretical but relevant concept that connects the administered dose with the actual initial concentration present in the circulation, determining the half-life of a drug [42]. The web server *ADME/TOX WEB* contains a predictive algorithm that generates a quantitative estimative of the apparent volume of distribution of a compound, based on physicochemical parameters, charge state, lipophilicity and hydrogen-bonding capacity. Results for our two proposals as well as Tipifarnib and Lonafarnib are summarized in Table 3.

3.5. Biological activity predictions

In order to analyze our proposals from a biological activity point view, predictions of biological activity spectra on the basis of their structural formulas were obtained using PASS. The set of pharmacological effects, mechanisms of action, and specific toxicities that might be exhibited by a particular compound in its interaction with biological entities, and which is predicted by PASS, is termed the "biological activity spectrum" of this compound [29]. This concept is crucial to *PASS* and that provides the rationale for predicting many biological activity types for different compounds. Within this concept, biological activity is

Table 3
Pharmacokinetic properties calculated for Tipifarnib, Lonafarnib and two proposals of FTase inhibitors.

Inhibitor	%*F*	%Maximum passive absorption	S_W (mg/mL)	%PPB	V_d (L/kg)	High-affinity P-gp substrate probability (%)	P-gp inhibitor probability (%)
Tipifarnib	30–70	2	<1	98.1	4.02	33.2	85.3
Lonafarnib	30–70	100	<0.1	99.6	3.47	47.9	93.9
Proposal 1	30–70	>70	>1	98.9	4.19	26.0	88.6
Proposal 2	30–70	>70	>1	99.8	6.16	26.3	89.4

considered to be an intrinsic property of the compound, depending only on its structure. Any "component" of this biological activity spectrum of a given compound is assumed to be detectable under suitable experimental conditions.

In *PASS*, chemical structure is described by original descriptors called Multilevel Neighborhoods of Atoms (MNA). It has been shown that the MNA descriptors are rather universal and are capable of representing various structure–property relationships, including many types of biological activity, mutagenicity and carcinogenicity, druglikeness, and others [44,45].

Based on the statistics of MNA descriptors for active and inactive compounds from the original training set, two probabilities are calculated for each activity: *Pa* – the probability of the compound being active and *Pi* – the probability of being inactive. Being probabilities, the *Pa* and *Pi* values vary from 0 to 1, and in general $Pa + Pi < 1$, since these probabilities are calculated independently. *Pa* and *Pi* can be considered to be measures of the compound under study belonging to the classes of active and inactive compounds, respectively, or can be seen as estimates for the first and second kinds of errors in the prediction.

The most probable activities for a given compound are characterized by *Pa* values close to 1, and *Pi* values close to 0 [29]. If a statistically significant set of samples with predictions obtained with the high threshold $Pa > 0.9$ is selected from a much larger database and assayed, one has to expect to lose 90% of the active compounds, but the fraction of false-positives will be very small. If a default cutoff of $Pa > 0.7$ is used, only 70% of the actives will be lost, but the fraction of false-positives will be a little bit higher. For $Pa > 0.7$, the compound investigated is very likely to reveal this activity in experiments, but in this case the chance of being the analogue of the known pharmaceutical agents for this compound is also high. On the other hand, *PASS* can be ideally applied to design new similar or derivative compounds, such as our proposals.

The result of prediction is presented as a list of activities with appropriate *Pa* and *Pi*, sorted in descending order of the difference $(Pa - Pi) > 0$. For Proposal 1, *PASS* predicts *Pa* and *Pi* values of 0.934 and 0.002, respectively, regarding to an antineoplastic activity via farnesyltransferase inhibition. For Proposal 2, *PASS* predicts *Pa* and *Pi* values of 0.980 and 0.001, respectively, regarding to an antineoplastic activity via inhibition of the same enzyme. In contrast, similar prediction performed for Tipifarnib reveals lower *Pa* and *Pi* values of 0.840 and 0.005, respectively, for the corresponding kind of activity. Predictions of antineoplastic activity were only obtained for these 3 compounds using the threshold $Pa > 0.7$, with highest difference $(Pa - Pi)$ indicated for Proposal 2.

Another important issue in designing novel drug candidates is toxicity. It is responsible for many compounds failing to reach the market and for the withdrawal of a significant number of them from the market after once they are approved. It has been estimated that 20–40% of failures in drug development can be attributed to toxicity concerns [42].

3.6. Toxicology and synthetic accessibility predictions

In silico prediction of toxicity has been performed in drug design and development in order to avoid the experimental study of potentially harmful substances. The expert system *DEREK* here used is able to predict carcinogenicity, mutagenicity and skin sensitization, and indicates the likelihood of a compound possessing such toxicities by classification into one of six categories, namely *certain*, *probable*, *plausible*, *implausible*, *improbable*, or *impossible* [31]. Only categories "certain" and "probable" being predicted for a particular compound are considered as a reason to stop its further study. On the basis of the *DEREK* prediction results, none toxicological end-point has been indicated for proposals 1 and 2, as well as Tipifarnib.

Apart from good ADMET properties, synthetic accessibility clearly plays an important role. The proposed structure has to be synthesized in order to undergo experimental *in vitro* testing to validate the activity predicted *in silico*. Several methods already exist for predicting synthetic accessibility, and *SYLVIA* here used is a scoring method that easily evaluates synthetic accessibility of structures based on structural complexity, similarity to available starting materials and assessment of strategic bonds where a structure can be decomposed to obtain simpler fragments. These individual components are combined to an overall score of synthetic accessibility by an additive scheme. The weights of the scoring function components are calculated by linear regression analysis based on accessibility scores derived from medicinal chemists [30].

In a few words, the molecular graph complexity score is a general indicator of topological and atom type composition complexity of the target structure. The method is based on graph and information theories and takes account of the size, symmetry, branching, rings, multiple bonds and heteroatoms of the target molecule. The ring complexity component of the scoring function penalizes bridged and fused ring systems that would give rise to synthetic difficulty. The stereochemical complexity is a simple counter of tetrahedral stereo centers of the target structure that contribute to poor synthetic accessibility [30].

Using a default threshold of 6, the scores obtained for proposals 1 and 2 were 5.76 and 5.71, respectively, whereas the corresponding score obtained for Tipifarnib was 5.84. This threshold specifies that compounds with overall synthetic accessibility score below the given value will be indicated as 'easy to synthesize'. This value can vary between 0 and 10, and should be lower than the upper bound threshold. Results obtained for our two proposals theoretically support their synthetic accessibilities.

Virtual screening simulations were also performed in order to search for additional promising novel lead molecules that could be able to interact with the active site of FTase similarly to Lonafarnib, i.e. only by intermolecular interactions, without coordinating the catalytic zinc ion. Diverse molecules with different scaffolds were thus selected, which show molecular features that elect them potential FTase inhibitors. Structures of the two top-ranked compounds selected by virtual screening are shown in Fig. 6, and results of simulations are shown in Fig. 7.

3.7. Docking simulations of the proposals

Docking simulations of proposals 3 and 4 showed three viable orientations of each compound within the FTase active site. Fig. 7b

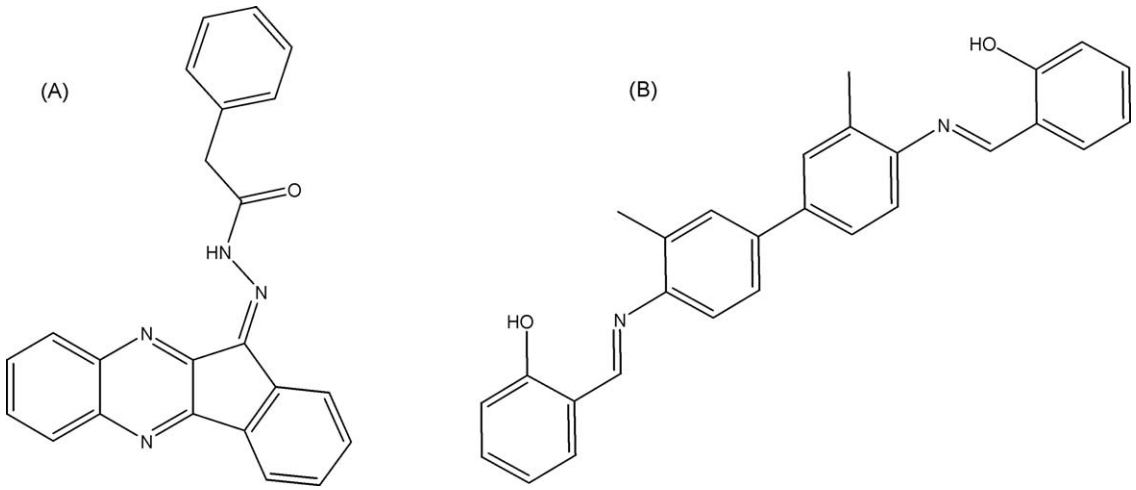

Fig. 6. Structures of the two top-ranked compounds selected by virtual screening. In (A), Proposal 3; in (B), Proposal 4.

shows the top-ranked orientation (score = 62.7) obtained for Proposal 3. Such orientation allows a hydrogen bond with Y361 (chain B) through its carbonyl oxygen. Regarding van der Waals interactions, W106 (chain B) and W102 (chain B) residues as well as the alkyl chain of FPP compose a favorable chemical environment to interact with the phenyl ring of Proposal 3. The condensed rings of such proposal could additionally to establish π-stacking interactions with the aromatic ring of Y361, whereas the benzoparadiazine moiety should be able to make van der Waals interactions with both W106 and D359 (Fig. 7).

Regarding the top-ranked orientation suggested with docking for Proposal 4 (score = 69.2), the two hydroxyl groups make hydrogen bonds with residues of the FTase active site (Fig. 8). One hydroxyl group interacts with R202 (chain B) residue, whereas the second hydroxyl is located in a favorable region between D297 (chain B) residue of FTase and the phosphate group of FPP. In addition, van der Waals interactions can be observed between one of the phenol rings of Proposal 4 and W102 (chain B), H149 and P152 (chain B) residues of the enzyme. Benzyl rings of such proposal make hydrophobic contacts with Y361 (chain B) and Y166 (chain A) residues of FTase.

3.8. Molecular dynamics simulations of the proposals

In order to evaluate the energetic and conformational stability of these two proposals inside the FTase active site, in presence of FPP, 1500 ps molecular dynamics simulations were subsequently performed with the corresponding top-ranked docking solutions obtained for Proposal 3 (Fig. 9) and Proposal 4 (Fig. 10). For such two proposals, which no coordinate zinc, no apparent conformational instability has been observed for each complex with FTase, such as indicated in the RMSDs vs. time plots, where low values of deviations of the molecules regarding their original atomic positions are observed. Our proposals theoretically thus preserve the main interactions pointed out in the docking simulations.

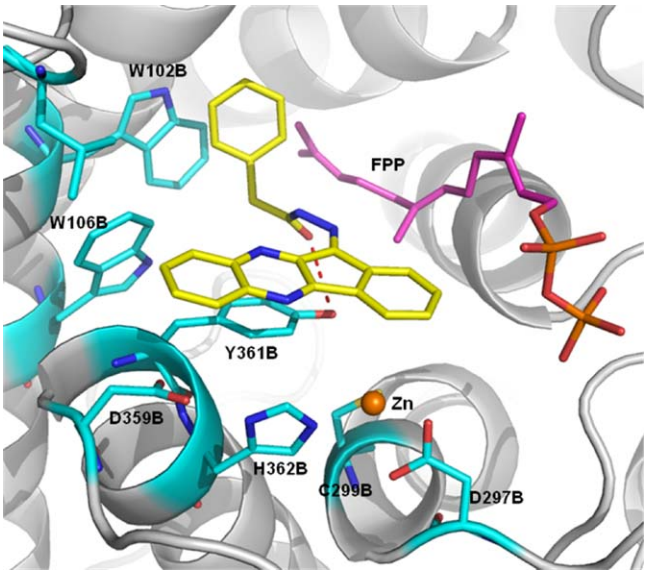

Fig. 7. Binding mode suggested by docking for Proposal 3 (carbon atoms are represented in yellow) is shown inside the FTase active site (selected residues are shown with carbon atoms in cyan). (For interpretation of the references to color in this figure legend, the reader is referred to the web version of the article.)

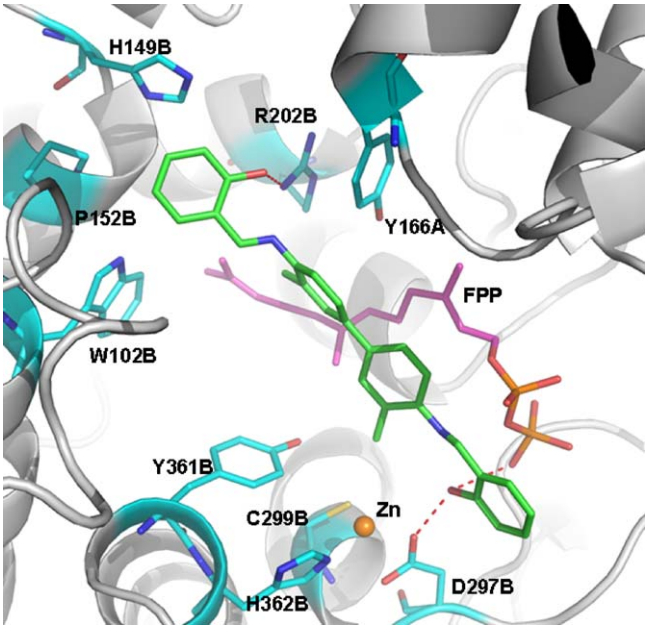

Fig. 8. Binding mode suggested by docking for Proposal 4 (carbon atoms are represented in yellow) is shown inside the FTase active site (selected residues are shown with carbon atoms in cyan). (For interpretation of the references to color in this figure legend, the reader is referred to the web version of the article.)

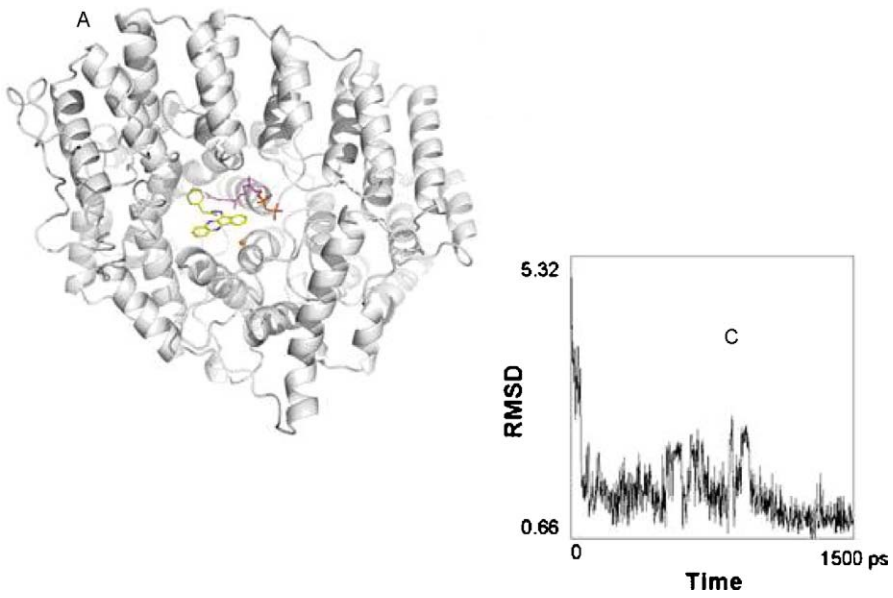

Fig. 9. In (A), top-ranked docking solution of Proposal 3 (carbon atoms in yellow) and FPP (carbon atoms in magenta) are shown inside the FTase active site. In (C), RMSD (in angstroms) of Proposal 3 is plotted as a function of time. (For interpretation of the references to color in this figure legend, the reader is referred to the web version of the article.)

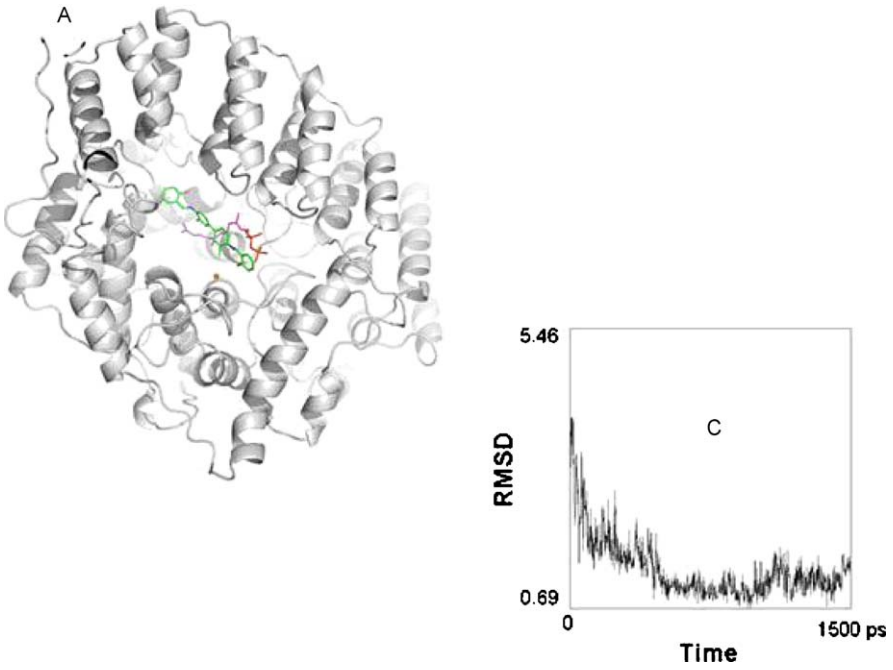

Fig. 10. In (A), top-ranked docking solution of Proposal 4 (carbon atoms in yellow) and FPP (carbon atoms in magenta) are shown inside the FTase active site. In (C), RMSD (in angstroms) of Proposal 4 is plotted as a function of time. (For interpretation of the references to color in this figure legend, the reader is referred to the web version of the article.)

4. Conclusion

We have used several computational chemistry methodologies to design and analyze four novel potential inhibitors of farnesyltransferase. Evaluation of proposals 1 and 2 regarding their drug abilities as well as lead compounds has indicated them as novel promisors FTase inhibitors when compared to the very active and most cited FTase inhibitors that have activity data reported, which are launched drugs or compounds in clinical tests. Proposal 1 appears to be a more promising drug candidate and FTase inhibitor than Proposal 2, but both derivative molecules indicate potentially very good pharmacotherapeutic profiles in comparison with Tipifarnib and Lonafarnib. Two other proposals have also been investigated by us, which suggest novel and alternatives scaffolds to design future potential FTase inhibitors. Such different compounds can be explored as promising molecules to start a research protocol in order to discover novel anticancer drug candidates targeting farnesyltransferase, in the fight against cancer.

Acknowledgements

We acknowledge financial support from CNPq, CAPES, FAPESP and FAPERJ.

References

[1] J.L. Bos, Ras oncogenes in human cancer: a review, Cancer Res. 49 (1989) 4682–4689.
[2] A. Gschwind, O.M. Fischer, A. Ullrich, The discovery of receptor tyrosine kinases: targets for cancer therapy, Nat. Rev. Cancer 4 (2004) 361–370.
[3] Y. Reiss, J.L. Goldstein, M.C. Seabra, P.J. Casey, M.S. Brown, Inhibition of purified p21ras farnesyl:protein transferase by Cys-AAX tetrapeptides, Cell 62 (1990) 81–88.
[4] K. Yokoyama, M.H. Gelb, Purification of a mammalian protein geranylgeranyltransferase: formation and catalytic properties of an enzyme–geranylgeranyl diphosphate complex, J. Biol. Chem. 268 (1993) 4055–4060.
[5] M.A. Vallim, L. Fernandes, J.A. Alspaugh, The RAM1 gene encoding a protein-farnesyltransferase b-subunit homologue is essential in Cryptococcus neoformans, Microbiology 150 (2004) 1925–1935.
[6] D. Qian, D. Zhou, R. Ju, C.L. Cramer, Z. Yang, Protein farnesyltransferase in plants: molecular characterization and involvement in cell cycle control, Plant Cell 8 (1996) 2381–2394.
[7] D. Caldelari, H. Sternberg, M. Rodriguez-Concepcion, W. Gruissem, S. Yalovsky, Efficient prenylation by a plant geranylgeranyltransferase-I requires a functional CaaL box motif and a proximal polybasic domain, Plant Physiol. 126 (2001) 1416–1429.
[8] D. Chakrabarti, T. Azam, C. del Vecchio, Y.L. Qiu, I. Park, C.M. Allen, Protein prenyl transferase activities of *Plasmodium falciparum*, Mol. Biochem. Parasitol. 94 (1998) 175–184.
[9] A.A. Adjei, An overview of farnesyltransferase inhibitors and their role in lung cancer therapy, Lung Cancer 41 (Suppl. 1) (2003) S55–S62.
[10] L. Vergnes, M. Peterfy, M.O. Bergo, S.G. Young, K. Reue, Lamin B1 is required for mouse development and nuclear integrity, Proc. Natl. Acad. Sci. U.S.A. 101 (2004) 10428–10433.
[11] A.D. Basso, P. Kirschmeier, W.R. Bishop, Thematic review series: lipid posttranslational modifications. Farnesyltransferase inhibitors, J. Lipid Res. 47 (2006) 15–31.
[12] D.L. Pompliano, M.D. Schaber, S.D. Mosser, C.A. Omer, J.A. Shafer, J.B. Gibbs, Isoprenoid diphosphate utilization by recombinant human farnesyl:protein transferase: interactive binding between substrates and a preferred kinetic pathway, Biochemistry 32 (1993) 8341–8347.
[13] E.S. Furfine, J.J. Leban, A. Landavazo, J.F. Moomaw, P.J. Casey, Protein farnesyltransferase: kinetics of farnesyl pyrophosphate binding and product release, Biochemistry 34 (1995) 6857–6862.
[14] W.R. Tschantz, E.S. Furfine, P.J. Casey, Substrate binding is required for release of product from mammalian protein farnesyltransferase, J. Biol. Chem. 272 (1997) 9989–9993.
[15] D.W. End, G. Smets, A.V. Todd, Characterization of the antitumor effects of the selective farnesyl protein transferase inhibitor R115777 in vivo and in vitro, Cancer Res. 61 (2001) 131–137.
[16] A.D. Cox, C.J. Der, Farnesyltransferase inhibitors: promises and realities, Curr. Opin. Pharmacol. 2 (2002) 388–393.
[17] E.J. Feldman, Farnesyltransferase inhibitors in myelodysplastic syndrome, Curr. Hematol. Rep. 4 (2005) 186–190.
[18] A.K. Ganguly, R.J. Doll, V.M. Girijavallabhan, Farnesyl protein transferase inhibition: a novel approach to anti-tumor therapy. The discovery and development of SCH 66336, Curr. Med. Chem. 8 (2001) 1419–1436.
[19] F.A. Eskens, A. Awada, D.L. Cutler, M.J. de Jonge, G.P. Luyten, M.N. Faber, P. Statkevich, A. Sparreboom, J. Verweij, A.R. Hanauske, M. Piccart, Phase I and pharmacokinetic study of the oral farnesyl transferase inhibitor SCH66336 given twice daily to patients with advanced solid tumors, J. Clin. Oncol. 19 (2001) 1167–1175.
[20] J. Woo, T.H. Nakagawa, A.M. Krecic, K.A. Nagai, D. Hamilton, S.M. Sebti, P.H. Stern, Inhibitory effects of mevastatin and a geranylgeranyl transferase I inhibitor (GGTI-2166) on mononuclear osteoclast formation induced by receptor activator of NF kappa B ligand (RANKL) or tumor necrosis factor-alpha (TNF-alpha), Biochem. Pharmacol. 69 (2005) 87–95.
[21] S.M. Sebti, Blocked pathways: FTIs shut down oncogene signals, Oncologist 8 (2003) 30–38.
[22] C.A. Taft, C.H.T.P. Silva, State-of-the-art of computer-aided drug design: an overview, in: C.A. Taft, C.H.T.P. Silva (Eds.), Current Methods in Medicinal Chemistry and Biological Physics, vol. 2, Research Signpost, Kerala, 2007, pp. 1–32 (International Invited MiniReview: C.A. Taft, V.B. Silva, C.H.T.P. Silva, Topics in Computer-aided Drug Design, J. Pharm. Sci. 97 (2008) 1089–1098).
[23] C.A. Taft, C.H.T.P. Silva, Invited international review: cancer and aids: new trends in drug design and chemotherapy, Curr. Comput. Aided Drug Des. 2 (2006) 307–324, and references therein.
[24] V.B. Silva, C.A. Taft, C.H.T.P. Silva, Use of virtual screening, flexible docking, and molecular interaction fields to design novel HMG-CoA reductase inhibitors for the treatment of hypercholesterolemia, J. Phys. Chem. A 112 (2008) 2007–2011.
[25] L.I.S. Hage-Melim, C.H.T.P. Silva, E.P. Semighini, C.A. Taft, S.V. Sampaio, Computer-aided drug design of novel PLA2 inhibitor candidates for treatment of snake bite, J. Biomol. Struct. Dyn. 27 (2009) 27–36.
[26] V.B. Silva, A.M. Namba, D.G. Pantalena, T.F. Prado, C.H.T.P. Silva, In silico search and toxicologic prediction of novel potential beta-secretase inhibitors in Alzheimer's disease, Curr. Bioact. Compd. 5 (2009) 119–127.
[27] A.M. Namba, V.B. Silva, T.M.B. Ramos, R.B. Vermelho, N.Z. Baptista, C.H.T.P. Silva, Virtual screening and toxicologic prediction of novel potential non-nucleoside HIV-1 reverse transcriptase inhibitors, Curr. Bioact. Compd. 5 (2009) 128–136.
[28] Discovery Studio ViewerPro, version 5.0, 2002, Accelrys Inc., San Diego, CA.
[29] V.V. Poroikov, D.A. Filimonov, W.-D. Ihlenfeldt, T.A. Gloriozova, A.A. Lagunin, Y.V. Borodina, A.V. Stepanchikova, M.C. Nicklaus, PASS biological activity spectrum predictions in the enhanced open NCI database browser, J. Chem. Inf. Comput. Sci. 43 (2003) 228–236.
[30] K. Boda, T. Seidel, J. Gasteiger, Structure and reaction based evaluation of synthetic accessibility, J. Comput. Aided Mol. Des. 21 (2007) 311–325.
[31] J.C. Dearden, M.D. Barratt, R. Benigni, D.W. Bristol, R.D. Combes, M.T.D. Cronin, P.N. Judson, M.P. Payne, A.M. Richard, M. Tichy, A.P. Worth, J.J. Yourick, The development and validation of expert systems for predicting toxicity, ATLA 25 (1997) 223–252.
[32] M.L. Verdonk, J.C. Cole, M.J. Hartshorn, C.W. Mulrray, R.D. Taylor, Improved protein-ligand docking using GOLD, Proteins: Struct. Funct. Gen. 52 (2003) 609.
[33] Gaussian 03, M.J. Frisch, G. W. Trucks, H.B. Schlegel, G.E. Scuseria, M.A. Robb, J.R. Cheeseman, J.A. Jr. Montgomery, T. Vreven, K.N. Kudin, J.C. Burant, J.M. Millam, S.S. Iyengar, J. Tomasi, V. Barone, B. Mennucci, M. Cossi, G. Scalmani, N. Rega, G.A. Petersson, H. Nakatsuji, M. Hada, M. Ehara, K. Toyota, R. Fukuda, J. Hasegawa, M. Ishida, T. Nakajima, Y. Honda, O. Kitao, H. Nakai, M. Klene, X. Li, J.E. Knox, H.P. Hratchian, J.B. Cross, C. Adamo, J. Jaramillo, R. Gomperts, R.E. Stratmann, O. Yazyev, A.J. Austin, R. Cammi, C. Pomelli, J.W. Ochterski, P.Y. Ayala, K. Morokuma, G.A. Voth, P. Salvador, J.J. Dannenberg, V.G. Zakrzewski, S. Dapprich, A.D. Daniels, M.C. Strain, O. Farkas, D.K. Malick, A.D. Rabuck, K. Raghavachari, J.B. Foresman, J.V. Ortiz, Q. Cui, A.G. Baboul, S. Clifford, J. Cioslowski, B.B. Stefanov, G. Liu, A. Liashenko, P. Piskorz, I. Komaromi, R.L. Martin, D.J. Fox, T. Keith, M.A. Al-Laham, C.Y. Peng, A. Nanayakkara, M. Challacombe, P.M.W. Gill, B. Johnson, W. Chen, M.W. Wong, C. Gonzalez, J.A. Pople, Gaussian, Inc., Revision A.1, 2003, Pittsburgh, PA.
[34] P.J. Goodford, Computational procedure for determining energetically favourable binding sites on biologically important macromolecules, J. Med. Chem. 28 (1985) 849–857.
[35] Insight II user Guide, 2005, Accelrys, San Diego, CA.
[36] C.A. Lipinski, F. Lombardo, B.W. Dominy, P.J. Feeney, Experimental and computational approaches to estimate solubility and permeability in drug discovery and development settings, Adv. Drug Deliv. Rev. 23 (1997) 3.
[37] Y. Hsieh, J. Chen, W.A. Korfmacher, Mapping pharmaceuticals in tissues using MALDI imaging mass spectrometry, J. Pharmacol. Toxicol. Methods 55 (2007) 193–200.
[38] C.L. Strickland, P.C. Weber, W.T. Windsor, Z. Wu, H.V. Le, M.M. Albanese, C.S. Alvarez, D. Cesarz, J. del Rosario, J. Deskus, A.K. Mallams, F.G. Njoroge, J.J. Piwinski, S. Remiszewski, R.R. Rossman, A.G. Taveras, B. Vibulbhan, R.J. Doll, V.M. Girijavallabhan, A.K. Ganguly, Tricyclic farnesyl protein transferase inhibitors: crystallographic and calorimetric studies of structure–activity relationships, J. Med. Chem. 42 (1999) 2125–2135.
[39] T.S. Reid, L.S. Beese, Crystal structures of the anticancer clinical candidates R115777 (Tipifarnib) and BMS-214662 complexed with protein farnesyltransferase suggest a mechanism of FTI selectivity, Biochemistry 43 (2004) 6877–6884.
[40] T.S. Reid, S.B. Long, L.S. Beese, Crystallographic analysis reveals that anticancer clinical candidate L-778,123 inhibits protein farnesyltransferase and geranylgeranyltransferase-I by different binding modes, Biochemistry 43 (2004) 9000–9008.
[41] I.M. Bell, S.N. Gallicchio, M. Abrams, L.S. Beese, D.C. Beshore, H. Bhimnathwala, M.J. Bogusky, C.A. Buser, J.C. Culberson, J.E. Davide, M. Hutchings, C. Fernandes, J.B. Gibbs, S.L. Graham, K.A. Hamilton, G.D. Hartman, D.C. Heimbrook, C.F. Homnick, H.E. Huber, J.R. Huff, K. Kassahun, K.S. Koblan, N.E. Kohl, R.B. Lobell, J.J. Lynch Jr., R. Robinson, A.D. Rodrigues, J.S. Taylor, E.S. Walsh, T.M. Williams, C.B. Zartman, 3-Aminopyrrolidinone farnesyltransferase inhibitors: design of macrocyclic compounds with improved pharmacokinetics and excellent cell potency, J. Med. Chem. 45 (2002) 2388–2409.
[42] H. van de Waterbeemd, E. Gifford, ADMET in silico modeling: towards prediction paradise? Nature 2 (2003) 192–204.
[43] E.H. Kerns, L. Di, Drug-like Properties: Concepts, Structure Design and Methods: from ADME to Toxicity Optimization, Academic Press, San Diego, 2008.
[44] A.A. Geronikaki, A.A. Lagunin, D.I. Hadjipavlou-Litina, P.T. Eleftheriou, D.A. Filimonov, V.V. Poroikov, I. Alam, A.K. Saxena, Computer-aided discovery of anti-inflammatory thiazolidinones with dual cyclooxygenase/lipoxygenase inhibition, J. Med. Chem. 51 (2008) 1601–1609.
[45] A.A. Geronikaki, J.C. Dearden, D. Filimonov, I. Galaeva, T.L. Garibova, T. Gloriozova, V. Krajneva, A. Lagunin, F.Z. Macaev, G. Molodavkin, V.V. Poroikov, S.I. Pogrebnoi, F. Shepeli, T.A. Voronina, M. Tsitlakidou, L. Vlad, Design of new cognition enhancers: from computer prediction to synthesis and biological evaluation, J. Med. Chem. 47 (2004) 2870–2876.